Open access • Journal Article • DOI:10.1016/J.JQSRT.2011.09.013

Infrared emission spectroscopy of CO2 at high temperature. Part II: Experimental results and comparisons with spectroscopic databases — Source link

Sébastien Depraz, Sébastien Depraz, Marie-Yvonne Perrin, Marie-Yvonne Perrin ...+4 more authors

Institutions: Centre national de la recherche scientifique, École Centrale Paris

Published on: 01 Jan 2012 - Journal of Quantitative Spectroscopy & Radiative Transfer (Pergamon)

Topics: Emission spectrum, Spectroscopy, Radiative transfer and Hot band

Infrared emission spectroscopy of CO2 at high temperature. Part II: Experimental results and comparisons with spectroscopic databases

Sébastien Depraz, Marie-Yvonne Perrin, Philippe Rivière, Anouar Soufiani

Infrared emission spectroscopy of CO_2 at high temperature. Part II: Experimental results and comparisons with spectroscopic databases

S. Depraz[a,b,c], M. Y. Perrin[a,b], Ph. Rivière[a,b], A. Soufiani[*,a,b]

[a] *CNRS, UPR 288, Laboratoire EM2C, Grande Voie des Vignes, F-92290 Châtenay-Malabry, France*
[b] *École Centrale Paris, Grande Voie des Vignes, F-92290 Châtenay-Malabry, France*
[c] *ONERA, DEFA/MCTM, BP 72, F-92322 Châtillon, France*

Abstract

Measurements of CO_2 emission spectra at high temperature in the 2.7 μm and 4.3 μm regions are presented and compared to predictions from the spectroscopic databases, CDSD-4000 (Tashkun SA, Perevalov VI, JQSRT 2011; 112:1403-10) and HITELOR (Scutaru D et al, JQSRT 1994; 52:765-81). The measurements near 2.7 μm show that CDSD-4000 provides better agreement with experimental data, especially in the band wing corresponding to very hot band emission. In the 4.3 μm region, experimental intensities are generally lower than theoretical predictions but the measurements are more affected by the use of sapphire confinement tubes. The two spectroscopic databases provide closer results than in the 2.7 μm region although CDSD-4000 yields here also better agreement with experimental data in band wing. Analysis of the two spectroscopic databases is carried out in terms of vibrational and rotational energy cutoff and total band emissivities.

[*]Corresponding author. Tel.: + 33 1 41 13 10 71, fax: + 33 1 47 02 80 35
Email address: anouar.soufiani@em2c.ecp.fr (A. Soufiani)

Key words: FTIR emission spectroscopy, microwave plasma source, spectroscopic databases, high temperature CO_2 infrared radiation

1. Introduction

As discussed in the literature review presented in Part I [1], there is a lack of very high temperature measurements of CO_2 IR radiative properties. These measurements are useful to study the accuracy of spectroscopic databases when the latter are used in the extrapolation range of energy levels. We present in this second part FTIR emission measurements using a microwave post-discharge in CO_2 flow as emission source. The measurements are compared to predictions from spectroscopic databases including the recently published CDSD-4000 database [2] and the older HITELOR database [3].

Among the attempts to build approximate high temperature CO_2 spectroscopic databases, the HITELOR database has been developed for applications at medium to low spectral resolution and temperatures up to about 2500 K, corresponding to combustion applications. The HITRAN-1992 database was extended in the 2.7 μm, 4.3 μm and 12μm regions for the two major isotopologues $^{12}C^{16}O_2$ and $^{13}C^{16}O_2$. The intensities of the most important hot bands were calculated by pragmatic extrapolation of band intensities of the same type identified in HITRAN-1992. The extrapolations concerned the ν_3 transitions in the 4.3 μm region, the $\nu_1+\nu_3$ transitions near 2.7 μm, and the $\nu_3-\nu_1$ transitions in the 12 μm region. Vibrational energies were calculated by diagonalizing the vibrational Hamiltonian for each Fermi polyad with the spectroscopic constants of Ref. [4]. Hot lines were generated

for lower energy levels characterized by $v_1 \leq 10$, $v_2 \leq 10$ and $v_3 \leq 5$ and up to a rotational quantum number J=200, and were added to HITRAN-1992 lines.

In the Carbon Dioxide Spectroscopic Databank (CDSD), line positions and intensities are calculated from effective Hamiltonian and effective dipole moment operators. The parameters of these operators were adjusted to fit experimentally observed line positions [5] and intensities [6]. Three versions, CDSD-296 [7], CDSD-1000 [8] and CDSD-4000 [2] were successively developed and correspond to the temperature at which a cutoff in intensities of 1.0 10^{-27} cm molecule^{-1} was employed. The latest version CDSD-4000 contains about 628 million lines among which 574 million lines are for the main isotopologue. The maximum energy considered for this isotopologue is 43522 cm^{-1} and is close to the dissociation limit of the ground electronic state of CO_2.

In parallel to the development and improvement of the atmospheric HITRAN databank, a high temperature analogous databank, called HITEMP, has been developed for fewer molecules (H_2O, CO_2, CO, NO and OH) but encompassing many more bands and transitions than HITRAN. The 1995 version of the HITEMP databank [9] was based for CO_2 on a mix between HITRAN lines and DND calculations [10]. HITEMP-1995 predictions of CO_2 radiative properties were accurate in the 2 μm, 2.7 μm and 4.3 μm regions for temperatures up to about 1000 K but it was shown that they overestimate absorption at higher temperatures (see e.g. [11]). The latest version, HITEMP-2010 [12] is mainly constituted for CO_2 of an updated version of CDSD-1000 databank including an improvement of $^{13}CO_2$ data and lines of

three less abundant isotopologues.

For the very high temperatures considered in this study, we will compare the experimental results with the predictions from HITELOR and CDSD-4000 databanks. In addition to line positions and intensities provided in these databanks, one needs the internal partition sum (discussed in Sec. 4) and line shapes to perform line by line calculations to be compared to the measurements. We use here Voigt line shapes with the collisional broadening parameters of Ref. [13] for HITELOR and the semi-classical calculations of Ref. [14], also provided in CDSD-4000, when this databank is considered. A line wing cutoff of 50 cm^{-1} was found sufficient and was used in all the present calculations.

The paper is organized as follows. A discussion on experimental uncertainties is provided in Sec.2 and, then, the experimental results and the comparisons with theoretical predictions are presented for the 2.7 μm and 4.3 μm regions in Sec. 3. An intrinsic comparison between the two spectroscopic databases is finally performed and discussed in terms of energy cutoff and total band emissivities.

2. Experimental uncertainties

The first type of uncertainties is directly related to the measurement of CO_2 emission intensities and include confinement tube effects discussed in Part I [1], measurement calibration with a blackbody source, and other causes due to the experimental setup. But as one of the goals of this study is to compare the measured spectra to calculated ones, there is a second type of uncertainties resulting from the temperature distribution and CO and CO_2

molar fractions to be used in the calculations. As discussed in the first part, CO emission bands Δv=2 are used to determine the local temperature and CO molar fraction, but this emission becomes very weak on the periphery of the plasma and the temperature field has to be extrapolated in these regions.

Concerning the experimental uncertainties, we have analyzed the following points:

- the spatial resolution of the measurements is about 2 mm and spatial convolution may affect the results. A numerical simulation of this effect has been undertaken. The temperature profile measured with sapphire tubes at the height h=6 mm was used as input to compute CO line of sight integrated emission spectra. These spectra were then spatially convolved and Abel inverted. The temperature profile obtained from these convolved spectra was then compared to the initial one. This numerical simulation showed that temperature differences as high as 250 K are observed at the plasma center but, for the region where CO_2 emission is significant (T <5000 K and r >1.5 mm), the spatial convolution induces temperature changes smaller than about 30 K.

- The uncertainty on the temperature of the blackbody source used to calibrate the emission signals is estimated to be about 5 K, although the instrument specifications indicate less than 3 K. A temperature difference of 5 K around 900 K induces variations of the Planck's function of about 1.6% at 2000 cm^{-1} and 3.3% at 3700 cm^{-1}. Measurements of blackbody emission at different temperatures showed also that the ratio of Planck's functions was recovered within $\pm$1.5%.

- The use of a fluoride window, normal to the optical path, at the end of the tube connecting the plasma cavity to the spectrometer, induced some Fabry-Pérot interferences with the highest amplitude of ±2.2% at the lowest wavenumbers (4.3 μm region). This configuration was nevertheless preferred to an inclined window since it allowed to minimize residual absorption by ambient air.

- The analysis of confinement tube effects shows that accurate corrections may be carried out except for the measurements in the 4.3 μm region where the plasma is optically relatively thick. Due to reflections by the sapphire tube interfaces, the measured intensity may be underestimated by up to 15%.

For the uncertainties holding on the temperature and concentration profiles, there are also several issues that have been analyzed:

- In the central part of the plasma, the good agreement between the temperature deduced from the normalized and absolute CO spectra indicates accurate determination of both the temperature and CO molar fraction. Carbon atom conservation in the mixture leads then to an accurate determination of CO_2 concentration as well. The major uncertainty comes from temperature extrapolation on the plasma periphery. Although it does not significantly affect CO_2 concentration which is practically equal to 1 below 2000 K, this extrapolation will induce important uncertainties on the comparisons, especially for the peripheral chords, and in the spectral regions where the cold boundaries absorb significantly the radiation emitted by the central regions.

- The reliability of the CO spectroscopic data used in the least square adjustment of the temperature was checked by comparing different databases (see Part I). The uncertainties on CO line intensities were estimated to about ±2% for temperatures up to 7000 K.

- CO data analysis, including symmetrization, spatial filtering and Abel inversion introduces also uncertainties on temperature and concentration determination. We have checked by numerical simulation that uncertainties resulting from data processing remain of the same order than the uncertainties on the initial emission signals.

It appears from the above discussion that, except from the problem of sapphire tube effects in the 4.3 μm region, the major source of uncertainties is due to temperature and CO_2 concentration profiles, and particularly on the periphery of the plasma. Although this uncertainty concerns the calculated emission spectra, it is transformed, for figure legibility reasons, into error bars holding on the measured intensities. The temperature profile used in the calculations is the one deduced from the adjustment of the normalized CO spectra with linear extrapolation in the peripheral regions, and the height of the error bars is taken equal to the maximum difference between the spectra calculated using the four different temperature profiles, i.e. based on the normalized or absolute CO emission and using a linear or smooth extrapolation, with HITELOR database.

3. Experimental results and comparison with theoretical data

Measurements were carried out for several heights h above the plasma cavity and several displacements y from the central chord with a step δy=0.5 mm.

We present in the following the results obtained for h=6 and h=20 mm. The experimental operating conditions for the experiments using quartz and sapphire confinement tubes are given in Table 1.

[Table 1 about here.]

The temperature profiles, as determined from CO normalized spectra and linear interpolations on the boundaries, are shown on Fig. 1 for the experiments with both quartz and sapphire confinement tubes. CO_2 and CO molar fractions deduced from local chemical equilibrium calculations are also shown on this figure. A very high temperature central region appears for h=6 mm and, for h=20 mm, diffusion, convection, and probably radiation processes lead to smoother temperature profiles. Due to the very low CO_2 concentration in the central region $r < 2$ mm at h=6 mm, CO_2 emission from this region corresponding to temperatures greater than typically 4500 K will not significantly contribute to the emission signal. The temperatures are slightly higher with the sapphire confinement tube due to the higher microwave injected power.

[Figure 1 about here.]

3.1. The 2.7 μm region

Figures 2 presents the experimental absolute measured and calculated intensities at h=6 and 20 mm, and for the chords y=0 (central chord), y=5, 10 and 15 mm with quartz confinement tubes in the 2.7 μm region. Figure 3 shows the results for the same positions obtained with a sapphire confinement

tube. For legibility reasons, the experimental and calculated intensities are presented at low spectral resolution. A simple convolution with a 10 cm^{-1} wide rectangular function was used. The general trends and conclusions from quartz and sapphire experiments are similar.

It is first observed that the error bars are greater for the peripheral chords corresponding to low temperature levels and to the highest uncertainties on the temperature. For the central chords, the error bars are also more important in the spectral regions corresponding to "cold" lines, e.g. 3400–3750 cm^{-1} typically.

Though the error bars are very important for y=15 mm for instance, a good agreement between experimental and theoretical results is observed. This shows that the linear extrapolation of the temperature profile is a reasonable approximation and that both spectroscopic databases are reliable in the 2.7 μm regions for temperatures below typically 2000 K. Indeed, the results from HITELOR and CDSD-4000 are very close for y=10 and y=15 mm.

The results for central chords are more interesting since error bars are smaller and the contribution of high temperature regions to emission becomes predominant. The agreement between experimental data and theoretical predictions is obviously better with CDSD-4000, especially in the band wing (3000–3400 cm^{-1}) and for h=6 mm corresponding to higher temperature levels. Results from HITELOR underestimate clearly the emission in this spectral region, indicating that many "hot" lines are missing in this database. Note that for some chords, even CDSD-4000 results seem to be slightly outside the experimental error bars (Fig. 2, h=20 mm, y=10 mm and Fig. 3, h=6 mm, y=10 mm). In fact the error bars should be slightly larger since

they only take into account the uncertainties on the temperature profile and not the purely experimental uncertainties.

[Figure 2 about here.]

[Figure 3 about here.]

3.2. The 4.3 μm region

The measurements in the 4.3 μm region were carried out using sapphire confinement tubes since quartz absorbs and emits strongly in this region. The comparisons between experimental data and theoretical ones are shown on Fig. 4 for h=6 and 20 mm, and for the chords y=0 and y=5 mm. The errors bars are more important than those obtained in the 2.7 μm region, especially in the 2150–2400 cm^{-1} spectral range. This is due to the high optical thickness of the medium in this spectral range and to the important absorption by the cold layers of radiation emitted in hotter central regions. It should be noted that the difference between the results from the two spectroscopic databases are less pronounced than those observed in the 2.7 μm region.

However, the experimental results obviously underestimate the theoretical ones, except for the band wing where a good agreement is observed between experiments and CDSD-4000 calculations. The underestimation is more important at h=6 mm than at h=20 mm. It may be partly explained be sapphire tube effects discussed in detail in the first part [1]. For the high optical thicknesses of the 4.3 μm band, reflection by tube interfaces of the radiation propagating towards the spectrometer is not compensated by other symmetrical internal reflections. The resulting underestimation was estimated to

about 13% for τ_p=0.1. We recall that, in the optically thin band wing, a good agreement between CDSD4000 and experimental data is achieved. A rigorous treatment of tube effects requires the knowledge of plasma transmissivity at high spectral resolution, but absorption measurements in a wide spectral range are not an easy task at the very high temperatures considered in this study. Another solution would be the use of CO_2 diluted with a transparent species such as argon but this would result in a reduction of CO concentration and thus of the emission signal used to determine the temperature profile.

A pragmatic correction was attempted here. The experimental spectrum was simply multiplied by a function $f(\sigma)$ equal to 1.13 in the 2200–2400 cm^{-1} range and varying linearly between 1 and 1.13 in the range 1800–2200 cm^{-1}. The result of this pragmatic correction, given in Fig. 5, shows that experimental and calculation predictions are much closer though some discrepancies remain at the height h=6 mm.

[Figure 4 about here.]

[Figure 5 about here.]

In order to check the contributions of different regions in the plasma to the measured intensity on the central chord, partial intensities emanating from a given depth r (with -20< r <20 mm) were computed using CDSD-4000. Figure 6 shows the emission of the column (r, R) of the central chord with R=20 mm being the abscissa at the exit of the emitting column. The temperature profiles measured with a sapphire tube, shown on Fig. 1, were used for the simulation. It appears that the contribution of the region 8<

r <12 mm, corresponding to temperatures between 2500 K and 3000 K, is predominant in band wings (below 2100 cm^{-1} in the 4.3 μm region and 3300 cm^{-1} in the 2.7 μm region). The contribution of the region 4< r <8 mm, corresponding to temperatures typically between 3000 and 4000 K remains however significant in these band wings. In contrast, the contribution of the central region 0< r <4 mm is very weak, though visible for h=20 mm, due to the very small CO_2 concentrations. We may then conclude that the present experimental conditions allow us to check the validity of the spectroscopic databases up to roughly 4000 K.

[Figure 6 about here.]

3.3. High resolution comparisons

The experimental emission intensities presented above were measured with a Full-Width at Half-Maximum (FWHM) spectral resolution of about 0.10 cm^{-1}. They were then convolved at 10 cm^{-1} and compared to numerical predictions at the same resolution. Measurements with 0.016 cm^{-1} FWHM resolution were also carried out for the central chord after each experimental series. They allow us to study the quality of the spectroscopic databases in terms of extrapolated line positions. An estimation of the average FWHM CO_2 Voigt line profile at 3000 K leads to 0.03 cm^{-1} in the 4.3 μm region and 0.034 cm^{-1} in the 2.7 μm region. The high resolution spectral measurements are thus sufficient to resolve line profiles although there remains a small convolution effect with the apparatus function.

The comparisons between experimental spectra and CDSD-4000 predictions are shown on Fig. 7 for selected spectral regions and for the experiment at

h=20 cm with the sapphire tube. This experiment was selected because it provided a good agreement with CDSD-4000 at low spectral resolution for both 4.3 and 2.7 μm spectral regions. Four narrow spectral ranges were selected in band heads (around 2385 and 3761 cm^{-1}) and band wings (around 2118 and 3280 cm^{-1}) and, in the 4.3 μm region, attention was paid to select a region free from CO emission lines. To do this, calculations with and without CO contribution were compared. The only significant CO line in the selected narrow range of the 4.3 μm band wing is shown on the figure. It appears from Fig. 7 that a very good agreement between experimental and theoretical spectra is obtained in band heads. Due to the slightly different spectral resolutions, some differences are observed for the absolute signal levels but line positions are predicted very accurately. In contrast, in the band wings where emission arises from very hot lines, the agreement is less good and the spectra are not well correlated. This disagreement shows that the positions of very hot lines are not well predicted by CDSD-4000. However, the important density and overlapping of lines are so high that this issue should have no incidence in practical applications.

[Figure 7 about here.]

4. Comparisons between the spectroscopic databases

The aim of this section is to provide intrinsic comparisons between HITELOR and CDSD-4000 databases and to analyze the comparisons with experimental data given above. We discuss in a first step the vibrational and rotational energy cutoff in the two databases, then the difference between the internal partition functions used in association with each database, and conclude by

comparing predicted band total emissivities at different temperatures and optical paths.

Figure 8 shows the absorption coefficients calculated from the two databases at different temperatures and in the two spectral regions of interest. The high resolution calculations are convolved at 10 cm^{-1} spectral resolution. The agreement between the two predictions is good at 1000 K, satisfactory at 2000 K, and deteriorates gradually as the temperature increases. In order to fully understand this behavior, we have computed the cumulated distributions of line intensities of the main isotopologue $^{12}C^{16}O_2$ as a function of vibrational, rotational and total energy of the line lower level. These distribution functions are defined by:

[Figure 8 about here.]

$$\mathcal{F}(E''_r) = \sum_{line\, i/\, E''_{r_i} < E''_r} S_i(T), \quad (1)$$

$$\mathcal{F}(E''_v) = \sum_{line\, i/\, E''_{v_i} < E''_v} S_i(T), \quad (2)$$

$$\mathcal{F}(E''_{tot}) = \sum_{line\, i/\, E''_i < E''_{tot}} S_i(T), \quad (3)$$

where $S_i(T)$ is the intensity (in cm^{-2} atm^{-1}) of the line i at temperature T and E''_r, E''_v, E''_{tot} designate respectively the rotational, vibrational and total energy of the lower level. The cumulated distribution functions are shown on Fig. 9 in two spectral regions defined precisely by the 1800–2450 cm^{-1} and 2800–4400 cm^{-1} spectral ranges. As the vibrational levels in CDSD-4000 are denoted by a polyad index defined by $P = 2v_1 + v_2 + 3v_3$, we have roughly estimated E''_v by $P\omega_2$ where $\omega_2 \simeq 672$ cm^{-1} is the vibrational energy of the

mode ν_2. This leads to the small discontinuities shown on Fig. 9 for CDSD-4000 even for high vibrational levels. The vibrational energy for HITELOR was taken equal to the energy of the level having the smallest rotational quantum number within a given vibrational configuration.

At 2000 K, we observe reasonable agreement between the distribution functions predicted from the two databases in the two spectral regions. The total sum of line intensities predicted from HITELOR is however 15% smaller than the one predicted from CDSD-4000 in the 2.7 μm region. At higher temperatures, HITELOR leads to a higher total sum of line intensities in the 4.3 μm region, but to a significantly smaller one in the 2.7 μm region, when compared to CDSD-4000. A discontinuity in the derivative of the function $\mathcal{F}(E''_v)$ appears for the HITELOR database around E''=12700 cm^{-1} for the 4.3 μm region and E''=11000 cm^{-1} for the 2.7 μm region. This discontinuity is characteristic of a premature vibrational energy cutoff (see the description given in the introduction) and appears earlier in the 2.7 μm region, which explains the better global comparisons with experimental data in the 4.3 μm region. Although the rotational cutoff criteria correspond to J=200 in HITELOR and to J=300 in CDSD-4000, no discontinuity appears in the derivative of the function $\mathcal{F}(E''_r)$, which means that the rotational cutoff was less critical than the vibrational one.

The different internal partition functions used in association with the two spectroscopic databases constitute an additional explanation of the different band shapes observed on Fig. 8. Several high temperature partition functions of CO_2 have been reported in the literature [15–17]. They are compared on Fig. 10 for the main isotopologue $^{12}C^{16}O_2$. The partition function used

in HITELOR is the one tabulated by Gamache et al [15] and also used in HITRAN-1992. For CDSD-4000, Tashkun and Perevalov [2] use direct summation with the energy levels tabulated in their database. As the partition sum is not provided with a fine temperature step in Ref. [2], we have used in the present calculations with CDSD-4000 the simple uncoupled harmonic oscillators and rigid rotor function with a rotational constant B=0.3916 cm^{-1} and the vibrational wavenumbers ω_1=1353 cm^{-1}, ω_2=672 cm^{-1} and ω_3=2396 cm^{-1}. Figure 10 shows that this simple approximation leads to an excellent agreement with the partition function of Refs. [2, 17] up to 4000K. It shows also that the partition function used in HITELOR significantly underestimates the other calculations (5.8% at 2000 K, 25.6% at 3000 K and 43.5% at 4000 K in comparison with the direct sum used in CDSD-4000). This difference explains the band shapes observed at high temperature on Fig. 8 in the 4.3 μm region: HITELOR predictions overestimate the absorption coefficient in band center due to the underestimation of the partition function, but they underestimate absorption in band wing due to the vibrational energy cutoff.

[Figure 9 about here.]

[Figure 10 about here.]

The difference in the predicted band shapes may have important effects in practical radiation heat transfer calculations. We have computed for instance the total band emissivity defined by

$$\epsilon_t(T,l) = \frac{\int_{\sigma_1}^{\sigma_2}(1-\exp(-\kappa_\sigma l))I^0_\sigma(T)\,d\sigma}{\int_{\sigma_1}^{\sigma_2} I^0_\sigma(T)\,d\sigma}, \tag{4}$$

where l is the column length, $I^0_\sigma(T)$ is the Planck's function, and σ_1=1800 cm^{-1}, σ_2=2450 cm^{-1} for the 4.3 μm region, σ_1=2800 cm^{-1}, σ_2=4400 cm^{-1} for the 2.7 μm region. The results from HITELOR and CDSD-4000 are shown on Fig. 11 for different path lengths. As the optical thicknesses are much smaller in the 2.7 μm region than near 4.3 μm, a logarithmic scale is used in the first region. For small optical paths, good agreement between the two spectroscopic databases is observed in the 4.3 μm region whatever is the temperature. In contrast, important discrepancies are observed for high optical paths in the same spectral region due to emission saturation in band center and to the different band shapes. In the 2.7 μm region, HITELOR results systematically underestimate CDSD predictions at very high temperatures.

[Figure 11 about here.]

5. Conclusion

CO_2 IR emission spectra have been measured at very high temperature in the 2.7 and 4.3 μm regions using a microwave discharge in CO_2 flows and a high resolution FTIR spectrometer. Compared to tight cell measurements, further uncertainties resulted from the bad knowledge of the temperature distribution in the peripheral regions and from the use of a confinement tube, especially in the 4.3 μm region with sapphire tubes. Nevertheless, these measurements allowed us to study the validity and completeness of two spectroscopic databases, HITELOR and CDSD-4000. HITELOR database appears to be sufficient for classical combustion applications (for which it was intended during its construction), typically below 2500 K, and at low spectral resolution. At higher temperatures as those encountered for instance

in atmospheric entries, it is found to be insufficient due to the low energy cutoff of vibrational levels. CDSD-4000 yields generally very good agreement with experimental data, especially in band wings, indicating the reliability and the accuracy of this spectroscopic database for very high temperature applications. High spectral resolution comparisons revealed that very hot line positions are not accurately predicted in CDSD-4000. However, this fact should have no effects in practical applications due to the very high degree of line overlapping.

Acknowledgments

We acknowledge the French National Research Agency (ANR) for partial financial support through the project Rayhen and the funding from the European Community Seventh Framework Program under grant agreement 242311. We are grateful to Prof. S.A. Tashkun for providing us with CDSD-4000 databank prior to its publication.

References

[1] Depraz S, Perrin MY, Soufiani A. Infrared emission spectroscopy of CO_2 at high temperature. Part I: Experimental setup and source characterization. JQSRT 2011;Submitted.

[2] Tashkun SA, Perevalov VI. CDSD-4000: High-resolution, high-temperature carbon dioxide spectroscopic databank. JQSRT 2011;112:1403 –10.

[3] Scutaru D, Rosenmann L, Taine J. Approximate intensities of CO_2 hot bands at 2.7, 4.3 and 12 μm for high temperature and medium resolution applications. JQSRT 1994;52:765–81.

[4] Chedin A. Carbon-dioxide molecule - potential, spectroscopic, and molecular constants from its infrared spectrum. J Mol Spec 1979;76:430–91.

[5] Tashkun SA, Perevalov VI, Teffo JL, Rothman LS, Tyuterev VIG. Global fitting of $^{12}C^{16}O_2$ vibrational-rotational line positions using the effective Hamiltonian approach. JQSRT 1998;60:785 – 801.

[6] Tashkun SA, Perevalov VI, Teffo JL, Tyuterev VIG. Global fit of $^{12}C^{16}O_2$ vibrational-rotational line intensities using the effective operator approach. JQSRT 1999;62:571 –98.

[7] Tashkun SA, Perevalov VI, Teffo JL, Bykov AD, Lavrentieva NN. CDSD-296, the carbon dioxide spectroscopic databank: version for atmospheric applications. In: XIVth symposium on high resolution molecular spectroscopy. Krasnoyarsk, Russia, July 6-11; 2003,.

[8] Tashkun SA, Perevalov VI, Teffo JL, Bykov AD, Lavrentieva NN. CDSD-1000, the high-temperaure carbon dioxide spectroscopic databank. JQSRT 2003;82:165–96.

[9] Rothman LS, Wattson RB, Gamache RR, Schroeder J, McCann A. HITRAN, HAWKS and HITEMP high-temperature molecular data- base. Proc Soc Photo-Opt Instrum Eng 1995;2471:105 –11.

[10] Wattson RB, Rothman LS. Direct numerical diagonalization: Wave of the future. JQSRT 1992;48:763 –80.

[11] Bharadwaj SP, Modest MF. Medium resolution transmission measurements of CO_2 at high temperature-an update. JQSRT 2007;103:146–55.

[12] Rothman LS, Gordon IE, Barber RJ, Dothe H, Gamache RR, Goldman A, et al. HITEMP, the high-temperature molecular spectroscopic database. JQSRT 2010;111:2139 –50.

[13] Rosenmann L, Hartmann JM, Perrin MY, Taine J. Accurate calculated tabulations of IR and Raman CO_2 line broadening by CO_2, H_2O, N_2, O_2 in the 300-2400-K Temperature range. Appl Optics 1988;27:3902 –7.

[14] Bykov AD, Lavrentieva NN, Sinitsa LN. Semi-empiric approach to the calculation of H_2O and CO_2 line broadening and shifting. Molecular Physics 2004;102:1653 –8.

[15] Gamache RR, Hawkins RL, Rothman LS. Total internal partition sums in the temperature range 70–3000 K: Atmospheric linear molecules. J Mol Spec 1990;142:205 –19.

[16] Gamache RR, Kennedy S, Hawkins R, Rothman LS. Total internal partition sums for molecules in the terrestrial atmosphere. Journal of Molecular Structure 2000;517-518:407 –25.

[17] Osipov VM. Partition sums and dissociation energy for $^{12}C^{16}O_2$ at high temperatures. Molecular Physics 2004;102:1785 –92.

List of Figures

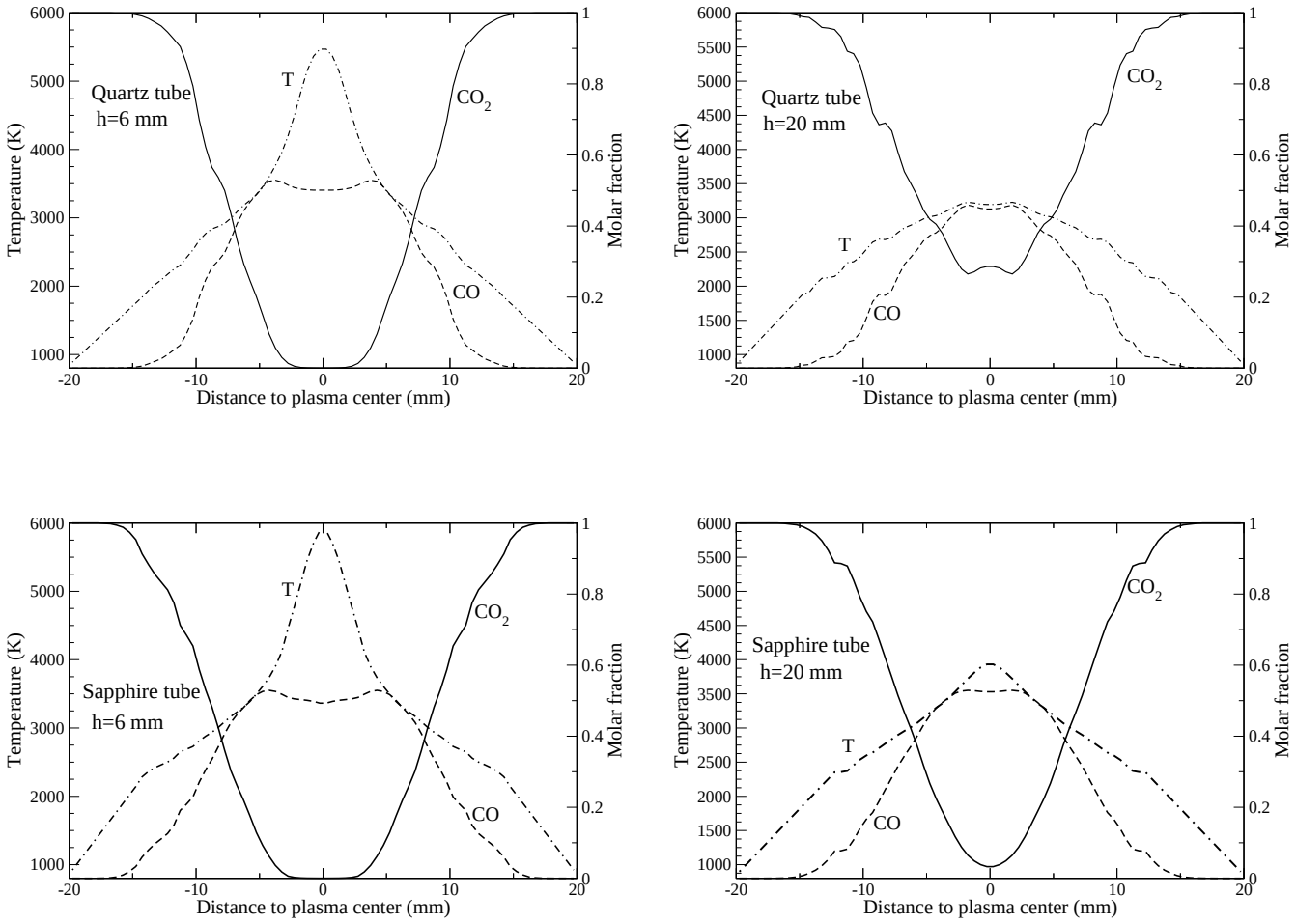

Figure 1: Temperature profiles deduced from CO normalized emission spectra with quartz and sapphire tubes at two heights h above the plasma cavity. CO and CO_2 molar fractions are deduced from calculations at local chemical equilibrium.

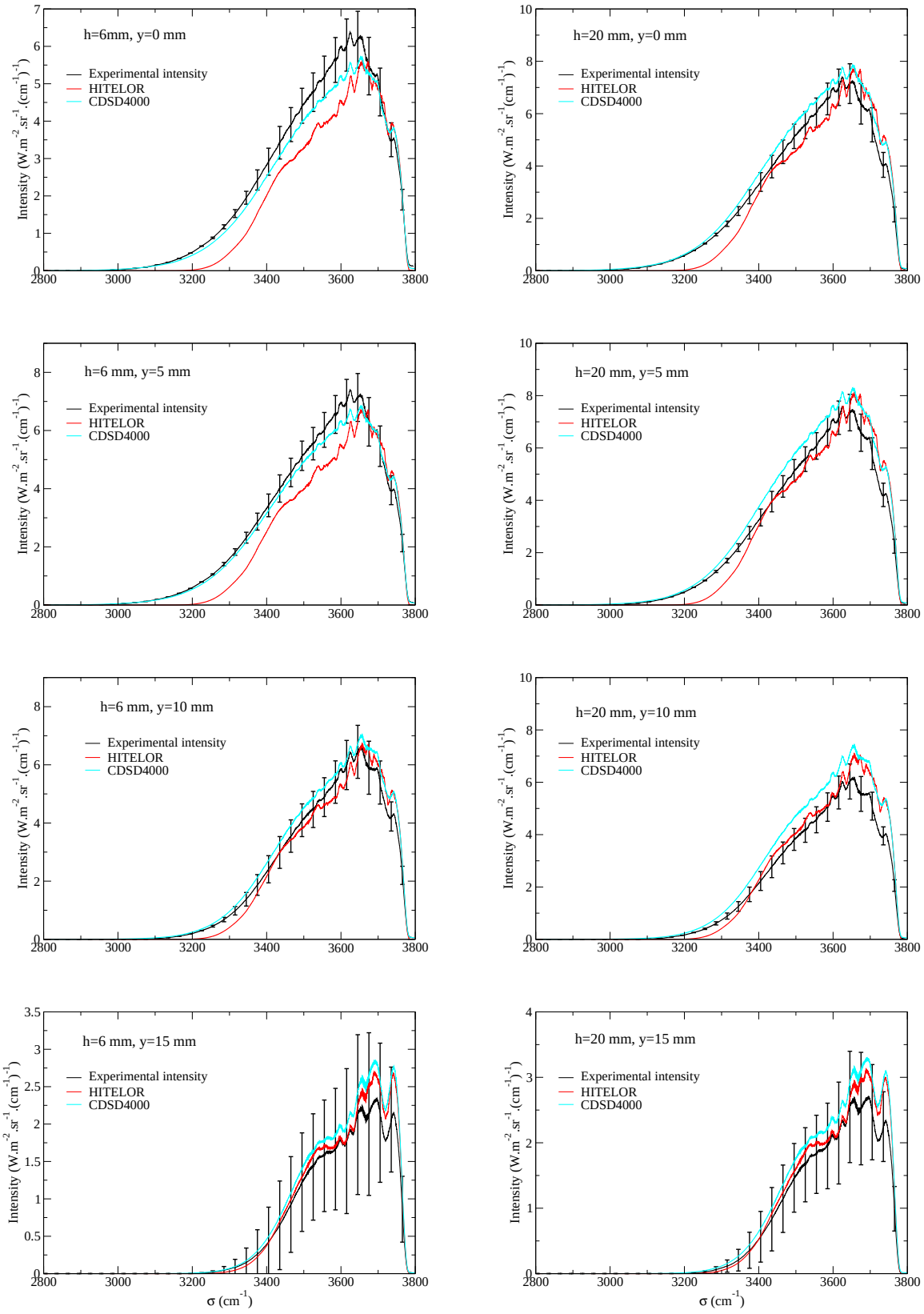

Figure 2: Experimental and theoretical line of sight integrated intensities at h=6 mm (left) and h=20 mm (right) and different distances y from plasma center; quartz tube; 2.7 μm region.

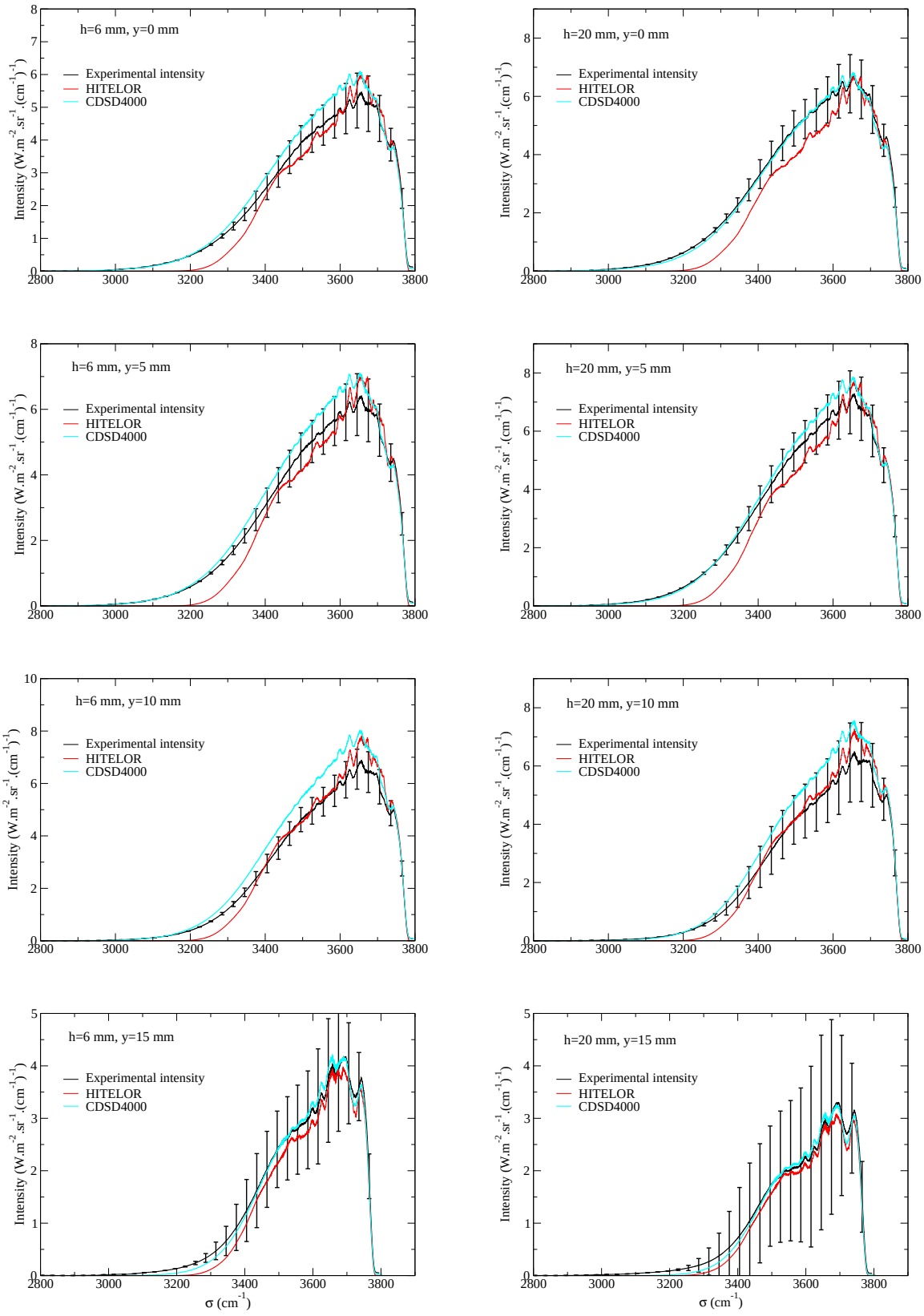

Figure 3: Experimental and theoretical line of sight integrated intensities at h=6 mm (left) and h=20 mm (right) and different distances y from plasma center; sapphire tube; 2.7 μm region.

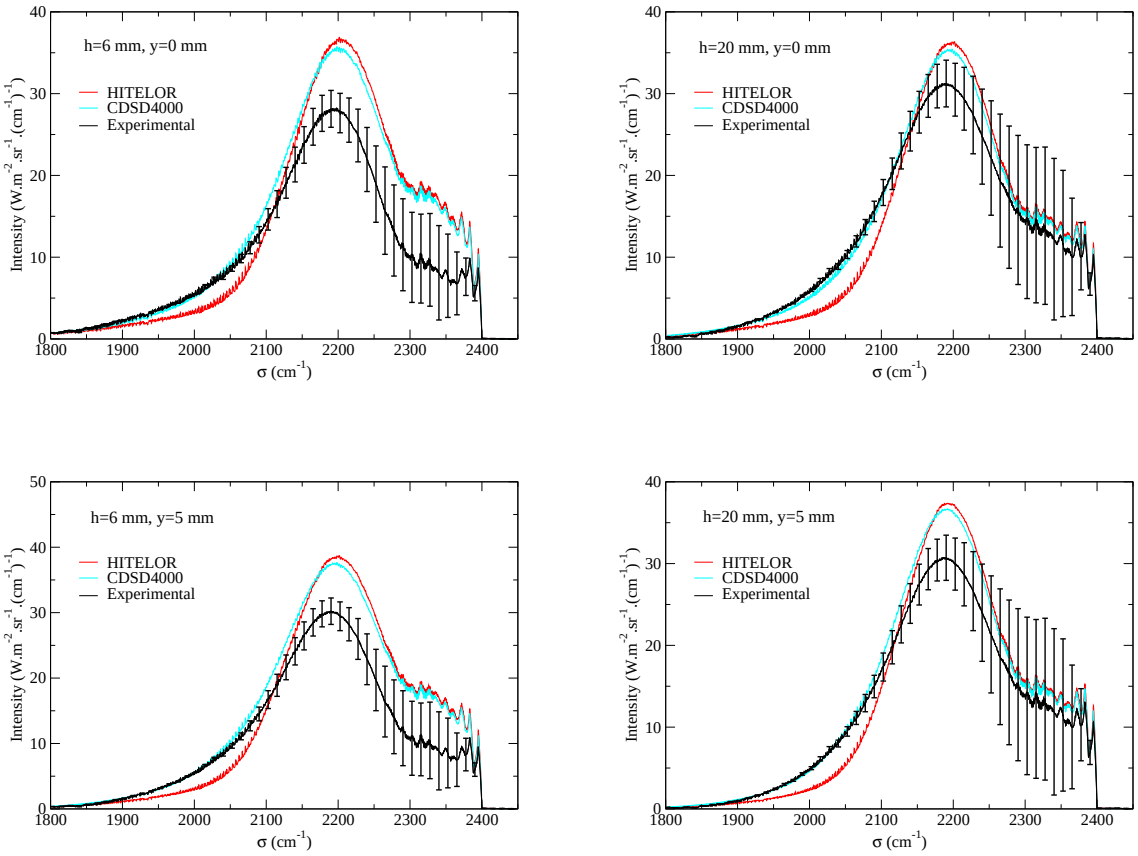

Figure 4: Experimental and theoretical line of sight integrated intensities at h=6 mm (left) and h=20 mm (right) and for y=0 (central chord) and y=5 mm ; sapphire tube ; 4.3 μm region.

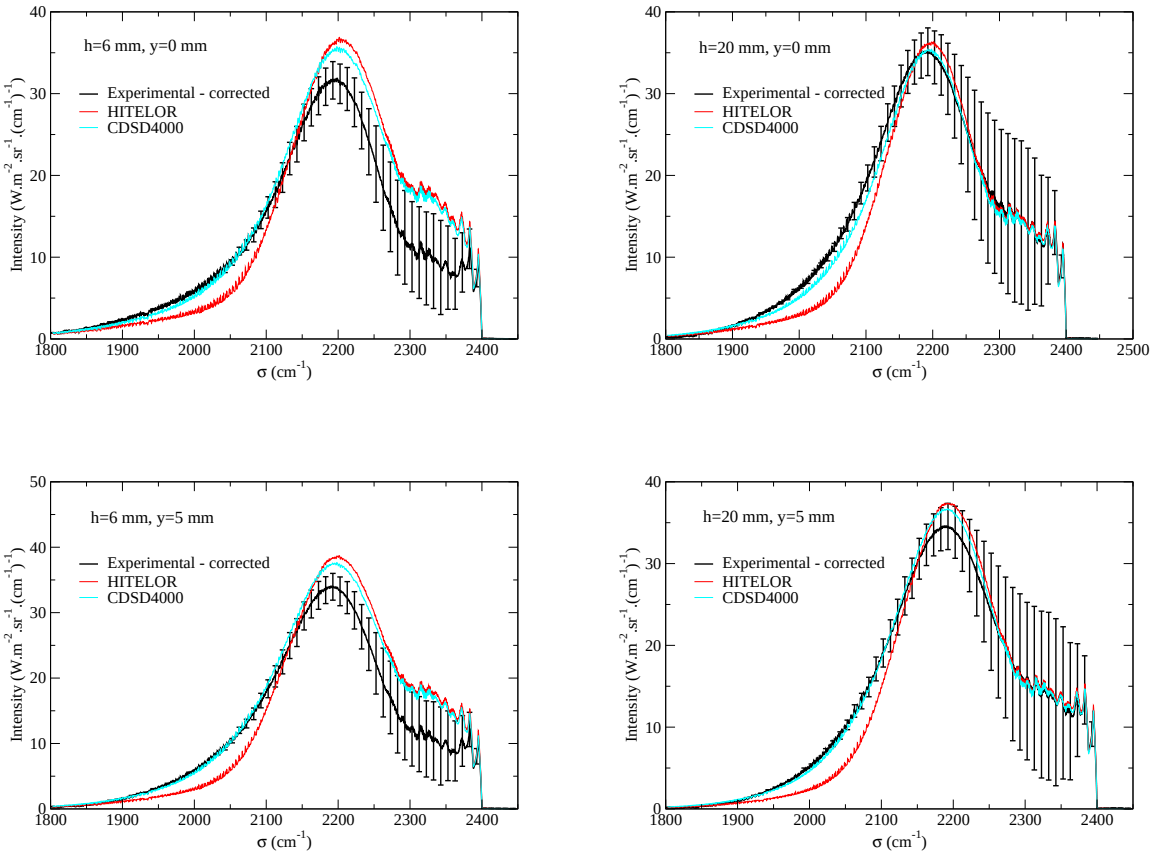

Figure 5: Experimental (corrected) and theoretical line of sight integrated intensities at h=6 mm (left) and h=20 mm (right) and for y=0 (central chord) and y=5 mm ; sapphire tube ; 4.3 μm region.

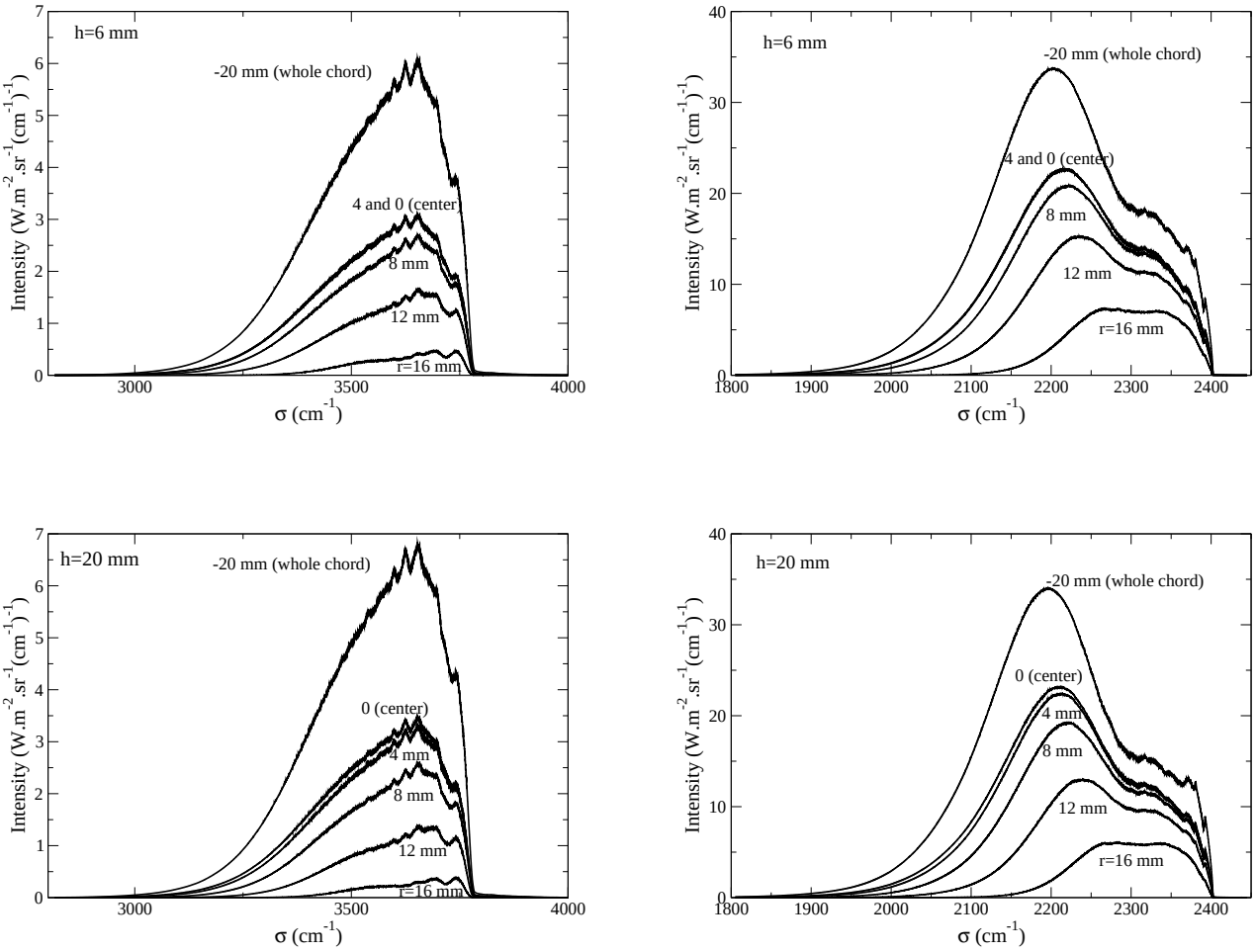

Figure 6: Partial intensities on the central chord computed with CDSD-4000 and the temperature profile obtained with a sapphire tube at h=6 mm and h=20 mm.

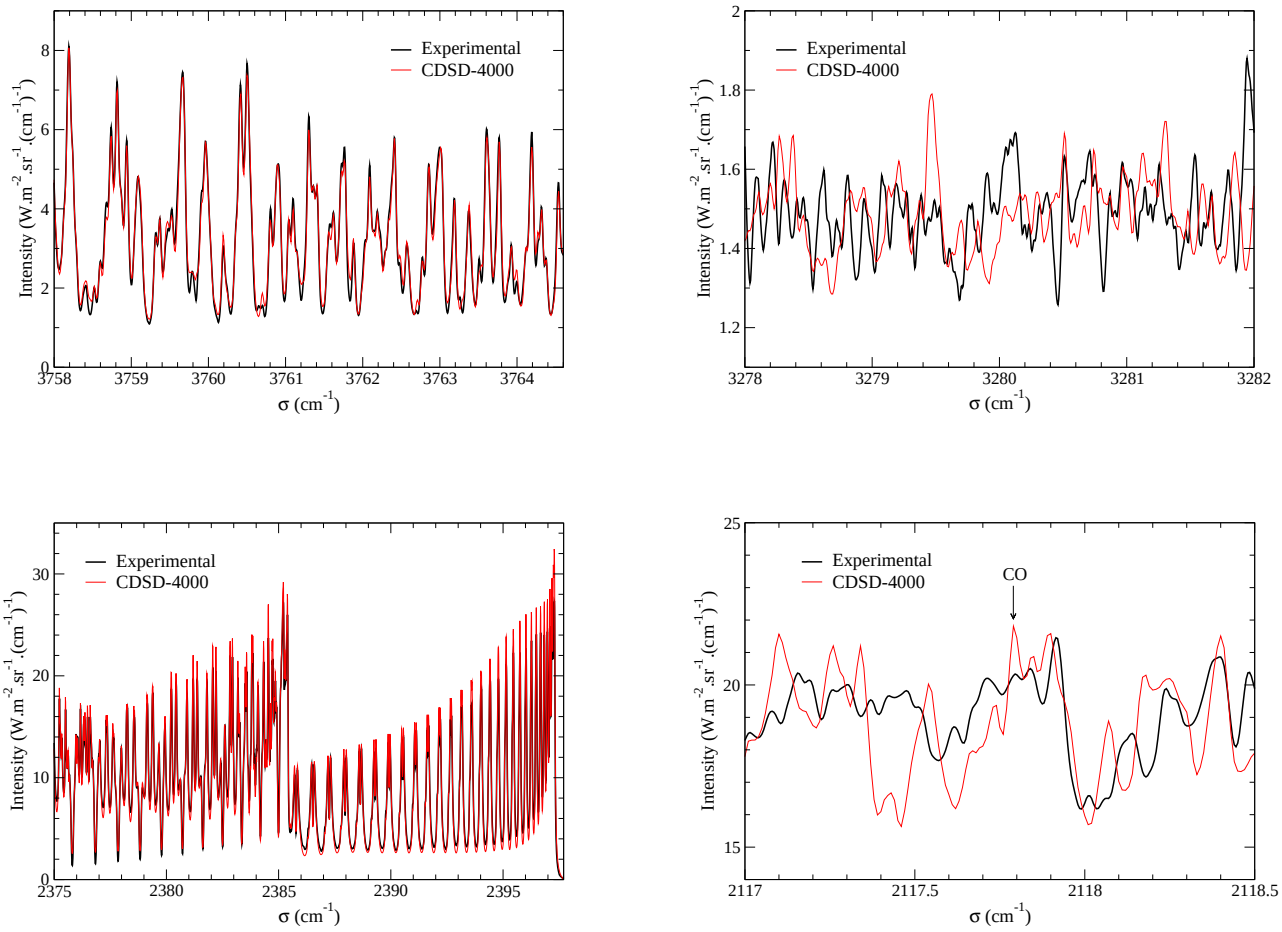

Figure 7: Comparison between high spectral resolution experimental intensities, obtained with a sapphire tube on the central chord at h=20 mm, and CDSD-4000 predictions in four selected spectral regions.

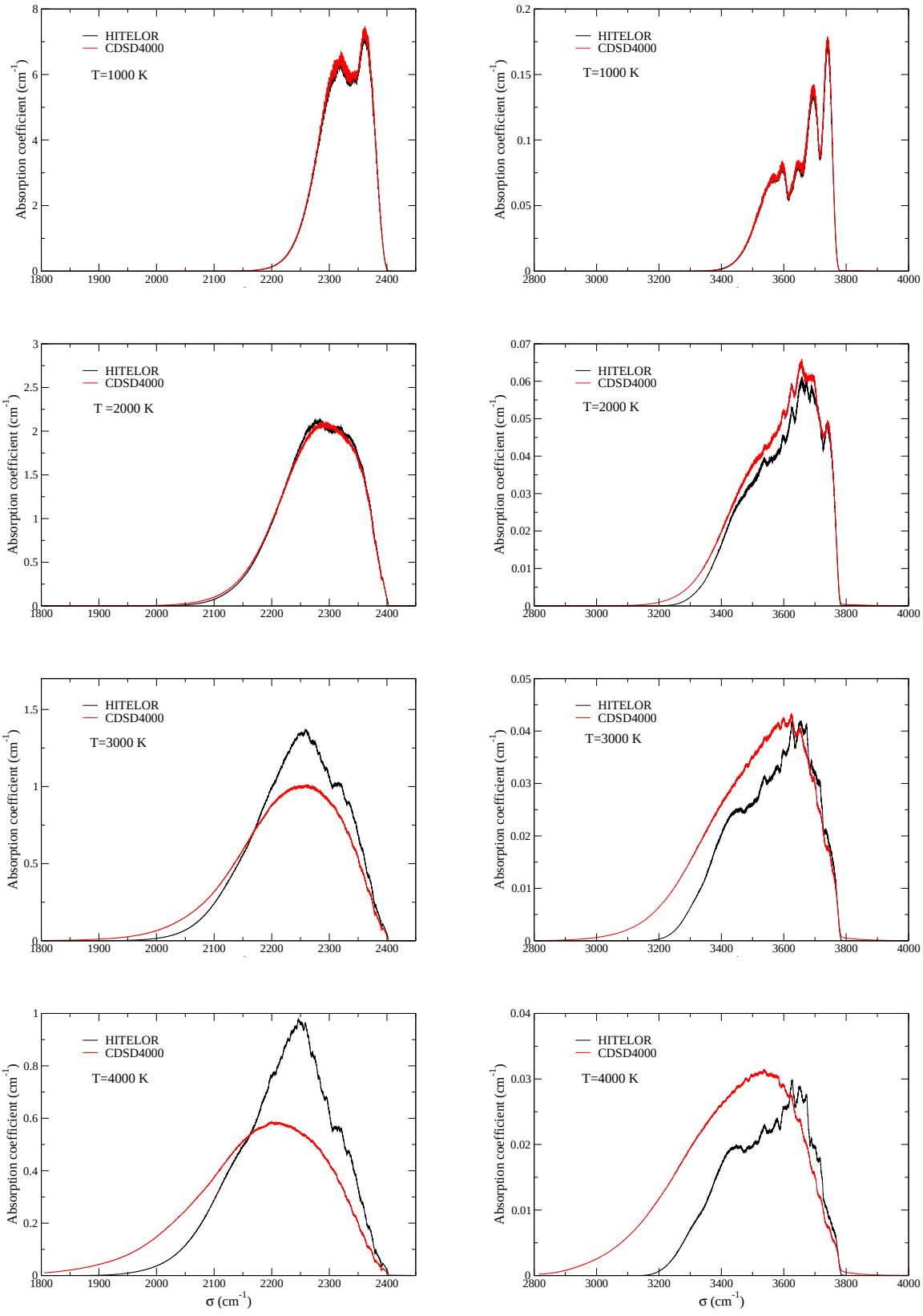

Figure 8: Pure CO_2 absorption coefficient at 1 atm and different temperatures.

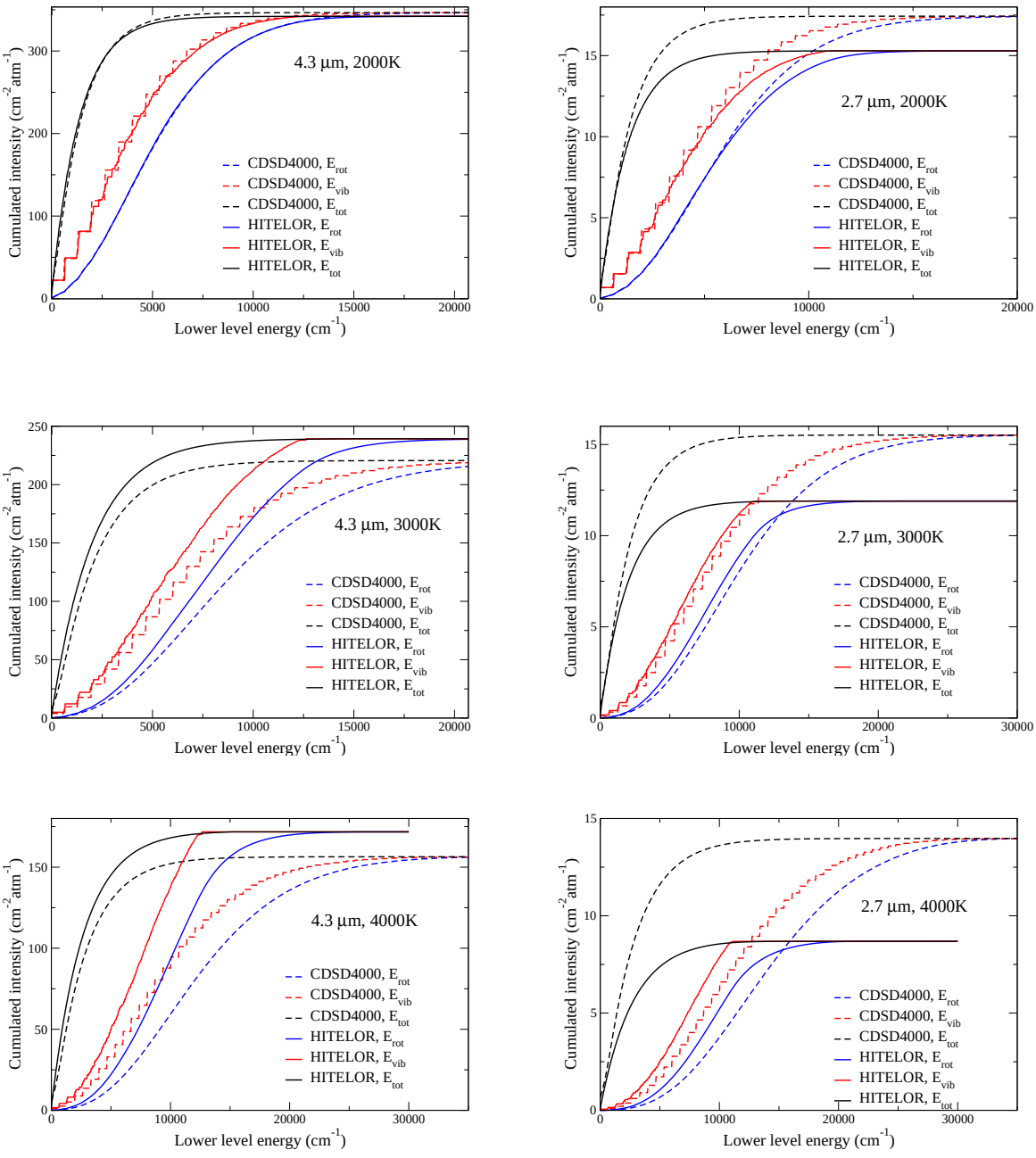

Figure 9: Cumulated distribution function of $^{12}C^{16}O_2$ line intensities vs lower level energy in the two spectral regions and for different temperatures.

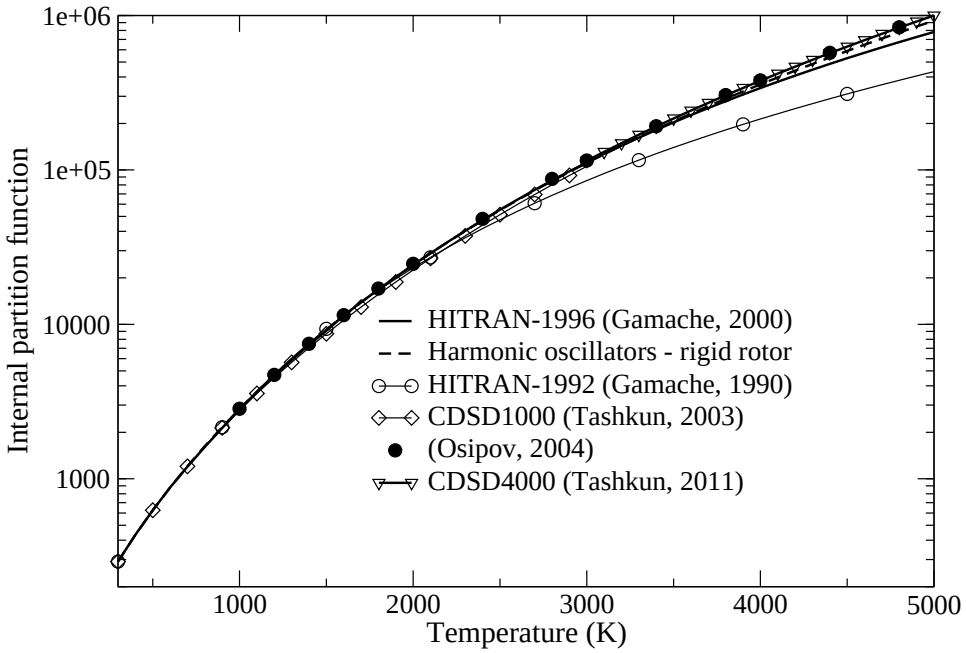

Figure 10: Internal partition sum of $^{12}C^{16}O_2$ according to different calculations.

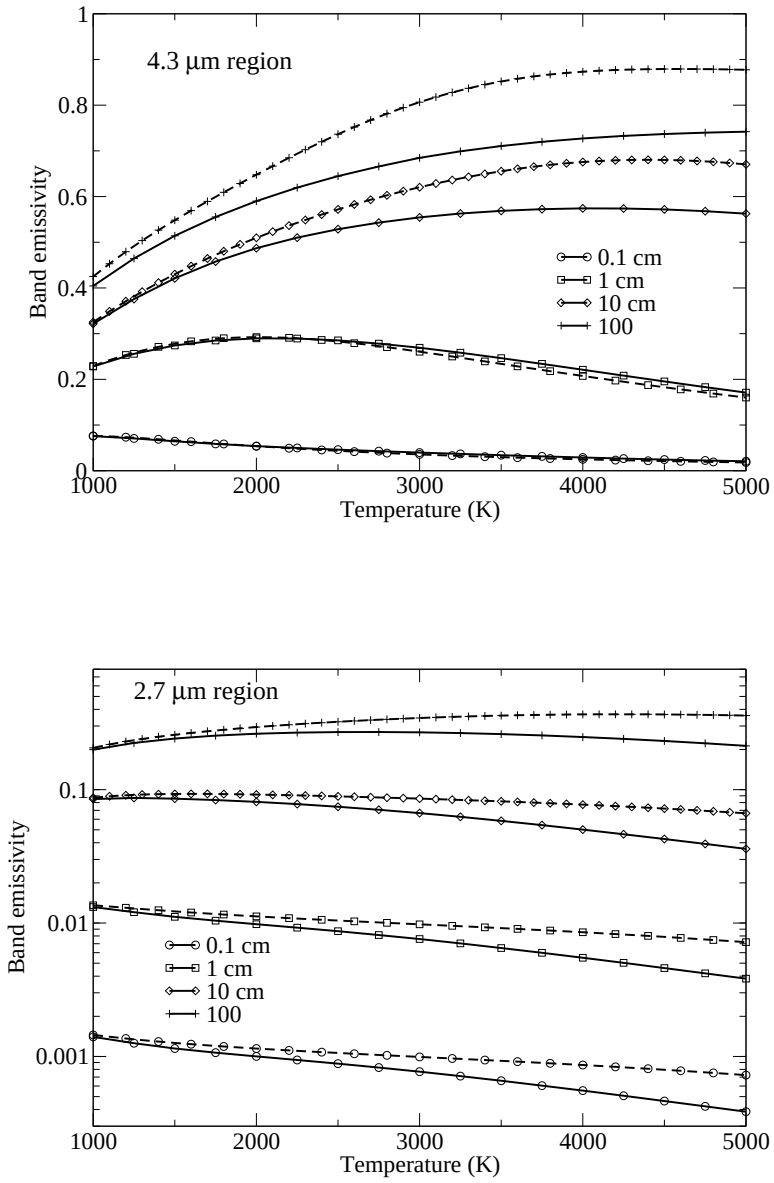

Figure 11: Total band emissivities of pure CO_2 at 1 atm as predicted from CDSD-4000 (dashed lines) and HITELOR (solid lines) in the spectral ranges 1800–2450 cm^{-1} (upper part) and 2800–4400cm^{-1} (lower part) for different column lengths.

List of Tables

Confinement tube	Quartz	Sapphire
Injected microwave power (kW)	1.00	1.35
CO_2 flow rate (l/mn)	7.00	7.00
N_2 purging flow rate (l/mn)	10.00	10.00
Spectrometer spectral range (cm^{-1})	1800–5000	1500–5500
Spectral resolution (FWHM, cm^{-1})	0.1	0.1
Number of interferogram scans	20	20
Apodization function	Hamming	Hamming
FTIR mirror velocity (cm/s)	1	1

Table 1: Experimental operating coditions.